ROV-based Tracking of a Shallow Water Nocturnal Squid

Samuel Yim, Christopher M. Clark
Engineering Department
Harvey Mudd College
Claremont, CA, USA
syim@hmc.edu, clark@hmc.edu

Timothy Peters, Vladimir Prodanov, Pat Fidopiastis
Computer Sci., Electrical Eng., Biological Sciences
California Polytechnic State University
San Luis Obispo, CA, 93405, USA
phphysics@gmail.com, vprodano@calpoly.edu,
pfidopia@calpoly.edu

Abstract — **This paper describes the use of a Remotely Operated Vehicle (ROV) equipped with a monocular vision system to find and track the squid *Euprymna scolopes*, so that motion behaviors of the squid could be characterized through the use of off-line image processing and state estimation. The ROV was deployed for several nights at several nearshore locations off Oahu, resulting in 10 hours of squid footage.**

Using blob-tracking image processing techniques and a Particle Filter state estimator, the squid can be detected and tracked. The position, velocity, and acceleration of the squid relative to the stationary ROV can be determined. Experiment results from tracking a simulated squid at known positions in a swimming pool and tracking of live squid in the ocean validate the performance of the tracking system. Results show the 3-D trajectory of the squid in a test feeding video. To the best of the authors' knowledge, this is the first observation and tracking of this species of squid in its natural environment.

Keywords – ROV, target tracking, squid, particle filter

Fig. 1. Shown in (a) is the Hawaiian squid *Euprymna scolopes* [Image courtesy of M.J. McFall-Ngai]. The VideoRay Pro III ROV is shown in (b).

I. INTRODUCTION

Within shallow-water coastal environments, there are a large number of animals, particularly small ones, for which we have little information regarding their daily behaviors, migratory paths, feeding patterns, etc. This list includes economically important animals such as crabs, shrimp and squid. This lack of knowledge is due primarily to the limited availability of technology capable of tracking these animals *in situ*. In this paper, we describe tools to track and monitor the behavior of small, shallow-water animals using the tropical squid, *Euprymna scolopes* (Fig. 1a), as a model.

Over the last two decades, *Euprymna scolopes* has emerged as a premier model for studying mechanisms of host-colonization by bacteria. Shortly after hatching, juvenile squid are colonized by cells of the luminous bacterium *Vibrio fischeri*. Once established, the bacterial population grows on squid-derived peptides, initiates dramatic morphological changes in squid tissue, and produces light. The importance of bacterial luminescence to these nocturnal squid is underscored by the fact that they possess accessory tissues such as a thick reflector to direct the light ventrally, an ink sac that is positioned to absorb stray light, and a muscle-derived lens to refract light into the environment.
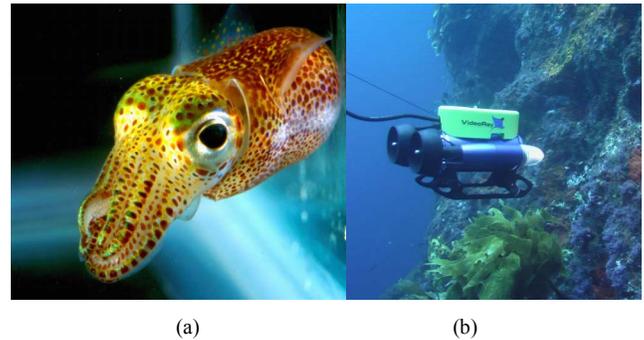
Despite the importance associated with understanding this species, and after two decades of laboratory studies ([1], [2], [3]) there is very little data on the behavioral and motion patterns of the squid within its natural environment.

This paper aims to characterize the behavior of *E. scolopes* in terms of the motion patterns, velocities, acceleration and distance covered during feeding. To accomplish this, the Remotely Operated Vehicle (ROV) shown in Fig. 1b, equipped with a video camera, was deployed in the shallow water beaches of Oahu, Hawaii. Two field expeditions that together spanned three weeks of nightly deployments resulted in 10 hours of video footage. Post-processing of this footage using standard image processing techniques and a particle filter has generated 3-D state estimates of various squid during feeding. In Section II, a background of underwater robotics and marine tracking are discussed. Section III describes the hardware setup and gives an overview of the problem. In Section IV, the state estimation that involves image processing and filtering techniques used for tracking squid are presented. Section V provides details of the experiments and results from both the Lab for Autonomous and Intelligent Robotics test pool, as well as the field deployments in Hawaii. Results from real tracking of squid are also discussed. Finally, Section VI gives a conclusion of the information discussed in this paper as well as future work on the topic.

II. BACKGROUND

Typically, biologists or scientists who sample in nearshore environments can accomplish their data acquisition via human divers, dredging from surface craft, attaching sensors to permanent moorings, using Remotely Operated Vehicles (ROVs), and recently using Autonomous Underwater Vehicles (AUVs). These methods have proven success in many scientific studies, but each has limitations.

There has been considerable interest in the use of Autonomous Underwater Vehicles (AUVs) [4] for applications like mapping. AUVs offer the advantage of a high degree of range of mobility due to their untethered operations at the cost of limited or no user interaction. A drawback of AUVs is that the underwater medium limits the transmission of video feedback to the surface, where ROVs can transmit video data through the tether. The tethers of ROVs, on the other hand, limit the range of the vehicle but allow users at the surface to send control signals to the ROV and receive sensor information in real-time.

Several methods have been developed to improve robot navigation capabilities of ROVs and AUVs, as well as to facilitate their use in biological sampling applications. Example approaches to mapping and navigation include the use of forward and downward-looking sonars [5], photo mosaics obtained from computer vision [6], and light section profiling [7].

Examples of biological sampling applications include [8], where an AUV was equipped with vision to investigate the bottom habitat. In [9], AUVs were used to aid in the study of near-shore bioluminescence. Of particular relevance is work done in [10], where an ROV was used to autonomously track jellyfish.

To facilitate the proposed studies in squid tracking and observation, an ROV was used to obtain video footage of the squid. Post-deployment image processing and filtering of the ROV obtained video must be accomplished to permit characterization of the squid's behavior. While the video data consists of rich environmental information such as color, texture, shape, dynamic properties and geometric properties etc., there are several issues that complicate image processing. Light attenuates exponentially with distance in water, which makes the quality of under-water images very poor, (see Fig. 5 for a representative frame). Feature extraction is complicated and can limit the possibilities for real-time implementation. Also, the vast array of unknown objects in the environment can be misinterpreted for the interested object.

In tracking fish specifically, several additional problems arise. The fish do not appear as exclusive bright against dark backgrounds. Illumination backscatters to the camera, producing a relatively bright and non-uniform background image. Suspended organic particles, known as marine snow, introduce continual small fluctuations to this background image. Finding gradients is also difficult with fish. Due to the difference of the light reflection ratio of fish scales, the intensity is uneven and the gradient distributions are scattered on the entire body, with some areas of strong intensity and others of weak intensity. Moreover, hotspots on the camera enclosure produce a strong gradient response. Lighting geometries that can result from these bright reflections are difficult to predict in advance. Color segmentation has success in extracting the fish from the water background, but encounters difficulties in separating the fish from seaweed and the seafloor.

Despite these issues, several papers have shown success in automated animal tracking in natural underwater environments, e.g. [10]. Clark et al. was successful in tracking tagged leopard sharks using a stereo-hydrophone system [11], [12]. Other researchers have automated visual extraction of marine animals from a video sequence, without closing servo loops. Widder et al. discuss vision techniques for on-line analysis of bioluminescent zooplankton data [13]. Fan and Balasuriya tested a 20 Hz fish tracking technique on-line, using video collected in the open ocean [14]. Other investigators have focused on pattern recognition methods useful for detecting underwater targets [15]. In [16], SIFT features were used to identify fish based on matching key SIFT features with an initial image of the fish.

In this project, several of these approaches have been attempted for tracking the Hawaiian squid *Euprymna scolopes*. As shown in [16], the relative bearing and depth of the target can be obtained, but the range cannot be determined from monocular vision alone unless the size of the squid is assumed. Here this size will be assumed, (but with low confidence or high variance), allowing full state estimation.

III. PROBLEM OVERVIEW

The goal of this project is to estimate the 3-D position of *E. scolopes* in its natural underwater environment using the RGB camera of a stationary ROV. Details of the hardware system and state estimation problem are described below.
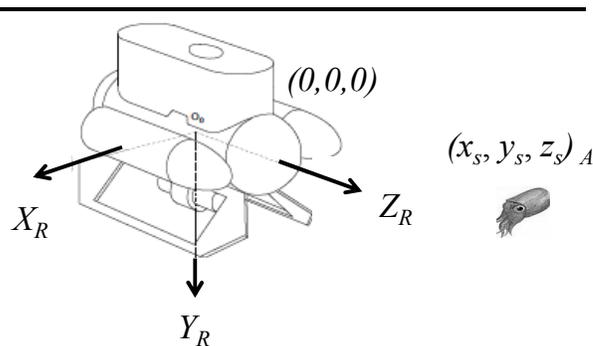

Fig. 2. The coordinate system used to represent the squid state.

A. ROV System Hardware

The VideoRay Pro III is a submersible vehicle remotely operated for underwater observation and exploration (Fig. 2). It has a depth rating of 150 meters, and is actuated with two forward thrusters and one vertical thruster. Its buoyancy and weighting tend to dampen out pitch and roll motion. The differential thrust configuration allows for rotation on the spot but no lateral motion.

The ROV sensors include one forward-facing color video camera, one rearward-facing black and white video camera, a compass and depth sensor. Two forward facing lights are mounted in front of the thrusters. A tether connects the ROV to a surface control box, allowing control signals (e.g. joystick commands) to be sent to the ROV and ROV sensor measurements (including video) to be sent in real-time to the control box. Additionally, the control box can be interfaced with an external computer for customized software control and processing of sensor measurements.

B. State Estimation Problem

Assume a stationary ROV at origin $(0, 0, 0)$ within the coordinate system (X_R, Y_R, Z_R) as shown in Fig. 2. Then, the absolute state of the squid is defined as the state of the squid relative to the ROV and is represented as $X_s = (x_s, y_s, z_s)_A$. The velocity and acceleration of the squid are denoted $V_s = (u, v, w)$ and $A_s = (u', v', w')$, respectively. The ROV receives N frames of video footage of the squid, where each frame is defined as the image I_0 at frame number t. This project seeks to use offline video processing to determine the position, velocity and acceleration of the squid over all frames during feeding. Formally,

Given: The set of N RGB frames containing squid

$$\mathbf{I} = \{ I_0^t \mid t \in (1, N) \}$$

Determine: The time parameterized squid trajectory states

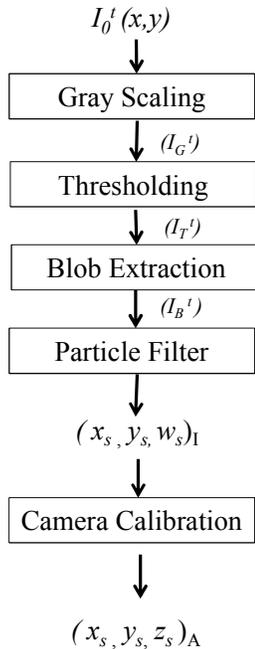$$\mathbf{X} = \{ [X_s \ V_s \ A_s] \mid t \in (1, N) \}$$

$$I_0^t (x,y)$$
↓
| Gray Scaling |
↓ (I_G^t)
| Thresholding |
↓ (I_T^t)
| Blob Extraction |
↓ (I_B^t)
| Particle Filter |
↓
$(x_s, y_s, w_s)_I$
↓
| Camera Calibration |
↓
$(x_s, y_s, z_s)_A$

Fig. 3. Overall system block diagram, with the final result $(x_s, y_s, z_s)_A$ the absolute coordinates of the squid's position.

(a)

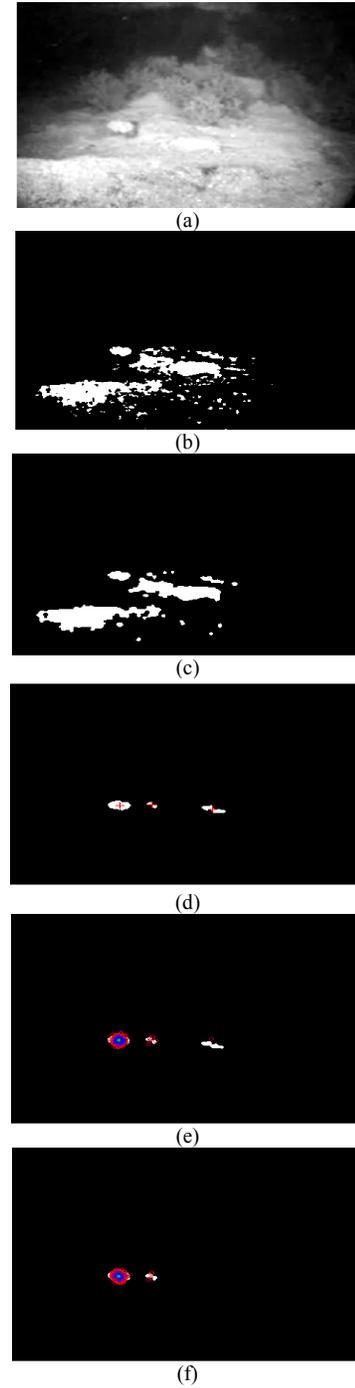
(b)

(c)

(d)

(e)

(f)

Fig. 4. X-Y state estimation algorithm. Shown in (a) is the grayscaled and adjusted video frame, with the squid visible in the left side of the image. Shown in (b) is the image after binary thresholding, and (c) shows the image after a disk-shaped structuring element is used to morphologically open and close the image. In (d) large and small areas are removed and the centroids of the final extracted blobs are marked. The particle filter converges on the squid blobs in (e) with the largest cluster around the actual squid. The following frame is shown in (f) where one of the potential squid blobs is shown to be noise from a different underwater object.

IV. STATE ESTIMATION ALGORITHM

Video footage of squid is processed offline in three steps. First, video images are grayscaled and converted to binary image frames via thresholding, a common approach discussed in more detail in [17], [18]. Correctly sized "blobs", or white labeled areas on a black background, are segmented in these binary image frames. Second, to account for disturbances and false positives due to lighting variance, the shallow-water environment, and various moving objects, a particle filter is implemented [19], [20]. This outputs the width as well as the X_R-Y_R pixel position of the squid. Lastly, the pixel position of the squid in each frame is used with a pixel-to-meter calibration of the ROV's camera to determine the absolute 2-D position of the squid, $(x_s, y_s)_A$, with respect to the stationary ROV. The absolute range, $(z_s)_A$, of the squid is found similarly, using the width of the squid with a width-to-range calibration of the ROV's camera. This process is summarized in the block diagram in Fig. 3 and described in more detail in the following sections.

A. Image Processing

The blobs are extracted from the squid footage using the method outlined in Fig. 4a-d. The squid footage obtained from the ROV's camera is grayscaled with increased contrast to obtain the image in Fig. 4a. To binarize the video frames, pixels above a brightness threshold are labeled white and those below are labeled black, (Fig. 4b). A disk-shaped structuring element is used to morphologically open and close the binary image. This removes noise in the background and foreground, and leaves only rounded objects, as shown in Fig. 4c. Finally, a size constraint on the blobs produces the final binary image in Fig. 4d. The blob sizes and locations are passed to the particle filter.

B. Particle Filter for X-Y Position Estimation

The particle filter takes as input a set of blob positions and sizes in pixel coordinates, where each blob is deemed a candidate squid position. The Particle Filter (PF) uses a collection of 1000 particles X^P to track the squid within the binary image. Each particle is defined by a state $[x\ y\ z\ u\ v\ w\ |\ w_i]$ in which the first three variables represent the 3-D position of the squid with respect to a Cartesian coordinate frame fixed on the camera with z being coincident with the cameras central axis and facing out of the camera lens (Fig. 2). The second three variables represent the associated velocity states, and the final variable w_i is the weight, that represents the likelihood that the particle state is the true state.

As shown in Algorithm 1, the PF iteratively updates the particle set for each time step, i.e. video frame t, using a prediction step and correction step [20].

1) Prediction Step - Each particle is first associated with the blob nearest to it, B_n, and has a velocity given by that blob's difference in position between frames, as shown in lines 2-5 of Algorithm 1. In lines 6-7, the particles are propagated forward according to a first order linear motion model with added randomness σ_{xy} based on the standard error of the squid's predicted position, (i.e. 5 pixels in this work).

Every iteration of the algorithm, 25% of the particles are randomly and uniformly distributed throughout the entire frame. That is, a k_p of 0.25 is used in lines 8-9 of Algorithm 1.

Algorithm 1 $\{X^P_t, w_s, [x^s_t, y^s_t]_1\} \leftarrow$ StateEstimator($\{X^P_{t-1}\}$, $I_{Bt}, \sigma_{xy}, \sigma_p, k_p$)

1:   //Prediction
2:   **for all** p particles **do**
3:       find nearest blob centroid B_n
4:       $u^p_{t-1} \leftarrow (x^{Bn}_{t-1} - x^{Bn}_{t-2})$
5:       $v^p_{t-1} \leftarrow (y^{Bn}_{t-1} - y^{Bn}_{t-2})$
6:       $x^p_t \leftarrow x^p_{t-1} + u^p_{t-1} + \text{randn}(0, \sigma_{xy})$
7:       $y^p_t \leftarrow y^p_{t-1} + v^p_{t-1} + \text{randn}(0, \sigma_{xy})$
8:       **for** k_p*p particles **do**
9:         $X^P \leftarrow$ RandUnif $\{\text{allPixelPositions}\}$
10:        $w^p_t \leftarrow$ h(D, σ_p)
11:   **end for**
12:
13:   //Correction
14:   $\{X^P\}_{temp} \leftarrow \{X^P\}$ for all p
15:   **for all** p particles **do**
16:       $\{X^P\} \leftarrow$ RandParticle($\{X^P\}, w^p_t$)
17:
18:   //Get Squid State
19:   **for all** blobs B **do**
20:       **for all** p particles **do**
21:         **if** p is nearest to B **then**
22:           $count(B)$ += 1
23:
24:   **for all** blobs B **do**
25:       **if** $count(B)$ **is max(***count(B)***) then**
26:         $[x^s, y^s]_1 \leftarrow$ **centroid**(B)   //pixel position
27:         $w_s \leftarrow$ **width**(B)
28:   **end for**

---

2) Correction Step – Particle weights are calculated based on their x-y Euclidean distance D to the nearest blob B_n as shown in (1) below. The standard deviation σ_p is the standard error in pixels between the blob tracking estimate of the squid's position and the actual pixel position of the squid, (determined experimentally as 8.8 pixels for this work).

$$h(D, \sigma_P) = \frac{1}{\sqrt{2\pi}\sigma_P} * e^{\left(\frac{-D^2}{2\sigma_p^2}\right)} \tag{1}$$

3) Get Squid State – Resampling typically results in several clusters of particles, each associated with one blob extracted from the image. For each image, the state of the squid $(x_s, y_s)_I$ is estimated as the centroid of the blob nearest to the largest cluster of particles, as shown in lines 20-30 of Algorithm 1. The centroid of a tracked squid is marked in Fig. 5. The width of the blob w_s is measured as the length of the minor axis of an ellipse drawn around it, (line 27).

Fig. 5. Actual squid footage from the ROV with a red dot marking the location of the squid estimated by the particle filter.

C. Camera Calibration

The position of the squid within the image can be converted from pixels to meters using a third order polynomial function created from a least squares fit to calibration data, shown in (1) – (6). The calibration data was created using a checkerboard grid pattern: known square locations in meters were fitted to manually measured pixel positions of the squares to find the calibration coefficients used in (4) and (5). Similarly, the calibration coefficients used in (6) were found by fitting the width of each square and its X position against the location of the square in the Z_R axis.

$$a = x_{pixel} \tag{1}$$

$$b = y_{pixel} \tag{2}$$

$$w = w_{pixel} \tag{3}$$

$$x_{meter} = c_{a,x}a + c_{b,x}b + c_{aa,x}a^2 + c_{bb,x}b^2 + c_{ab,x}ab + c_{aaa,x}a^3 \\ + c_{bbb,x}b^3 + c_{aab,x}a^2b + c_{abb,x}ab^2 + c_{a,x} \tag{4}$$

$$y_{meter} = c_{a,y}a + c_{b,y}b + c_{aa,y}a^2 + c_{bb,y}b^2 + c_{ab,y}ab + c_{aaa,y}a^3 \\ + c_{bbb,y}b^3 + c_{aab,y}a^2b + c_{abb,y}ab^2 + c_{a,y} \tag{5}$$

$$z_{meter} = c_{a,z}a + c_{w,z}w + c_{aa,z}a^2 + c_{ww,z}w^2 + c_{aw,z}aw + c_{aaa,z}a^3 \\ + c_{www,z}w^3 + c_{aaw,z}a^2w + c_{aww,z}aw^2 + c_{a,z} \tag{6}$$

V. EXPERIMENTS AND RESULTS

A. Swimming Pool

To validate the system, a truth data set was obtained by placing the ROV on the bottom of a swimming pool and recording video of a simulated squid object moving to known locations on a checkerboard grid (Fig. 6). This data set provided a known position of the object that could be compared against the estimated position to obtain a measurable error. Similarly, the grid was used to calibrate the size of an object and its X location in the camera image with respect to the absolute range of the object from the camera.

Fig. 6. Truth data test setup in a swimming pool.

It was determined that a significant source of error in range to the squid, z_s, was a result of inaccurate width measurements. 0 illustrates the difficulty in automatically determining the width of a squid in an image. Pixel widths of the grid squares were manually and automatically found for the first seven rows

of the grid, with the expectation that squares nearer to the camera and nearer to the middle of the grid would have larger widths. This was the case when accurate width measurements were made by hand (Fig. 7b), but not so when using the blob tracking algorithm (Fig. 7a) due to difficulties in clean blob extraction. Thus, to better characterize the tracking system, the errors of the state estimation algorithm were found for both automatically and manually determined widths. The results are summarized in TABLE I.
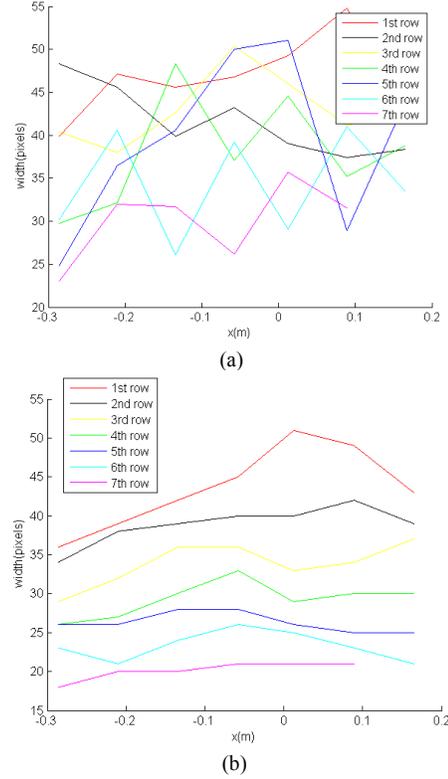

(a)

(b)

Fig. 7. Shown in (a) are the width measurements of the extracted squid blobs along each of the seven rows of the checkered grid, determined through image processing. Actual width measurements are shown in (b).

Fig. 8a shows the results of using the truth data to determine the errors of the state estimation algorithm when accurate width measurements are manually determined. The range measurements still have larger errors compared to the other two dimensions.

TABLE I. ERROR RESULTS IN SQUID TRACKING PARTICLE FILTER FOR AUTOMATICALLY AND MANUALLY DETERMINED WIDTHS

|	Widths from Particle Filter			Widths Manually Determined		
	mean error	*max error*	*standard deviation*	*mean error*	*max error*	*standard deviation*
x (m)	0.0109	0.0301	0.0162	0.0109	0.0301	0.0162
y (m)	0.00052	0.0017	0.00055	0.00052	0.0017	0.00055
z (m)	0.121	0.388	0.10	0.0238	0.0805	0.0304

To further validate the width-to-z calibration, a square trajectory was simulated along the checkered grid, and tracked. The known and estimated trajectories are shown in Fig. 8b.
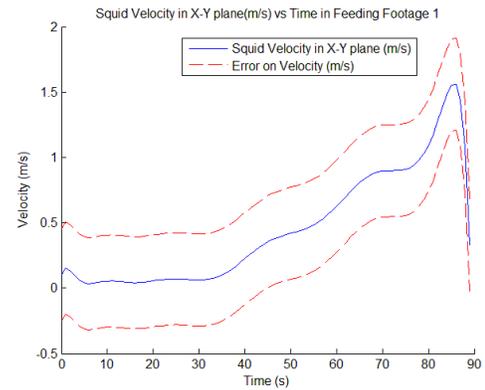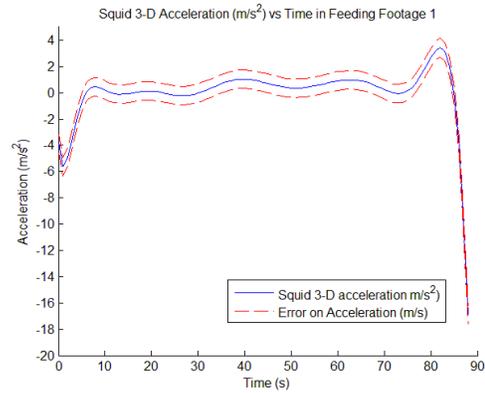
(a)

(a)

(b)

(b)
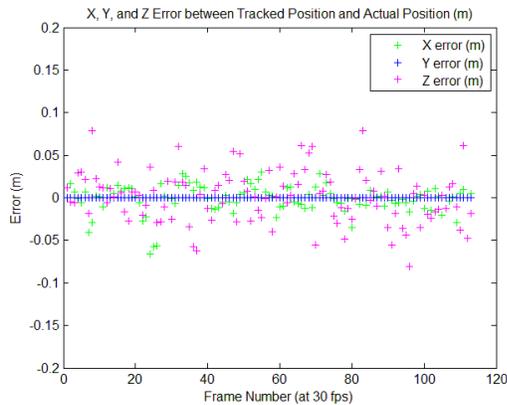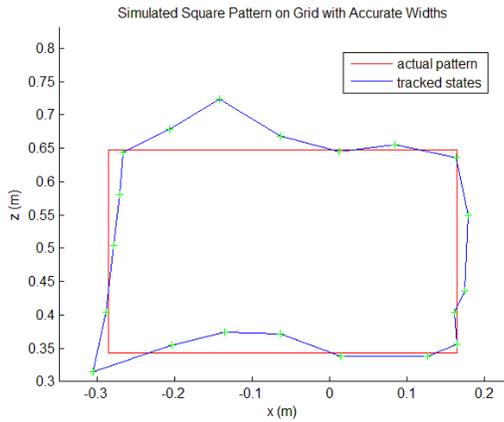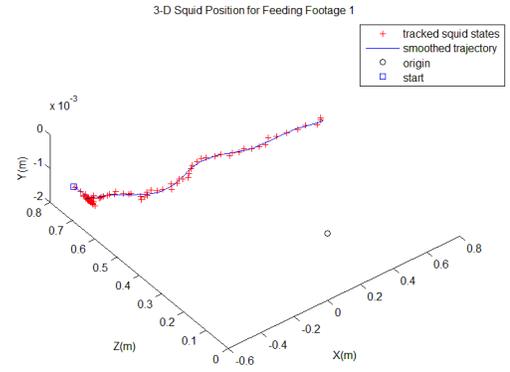
Fig. 8. Using accurate width dimensions. In (a), errors in x, y, and z direction in a truth test video. In (b), The red line is a simulated box pattern along a checkered grid, and the blue line is the pattern estimated using the tracked x coordinates and width-to-z camera calibration.

B. Oahu Shore

Actual footage from the ROV was obtained in waters near the shore of Oahu. The ROV was situated on the seafloor and captured footage of *E. scolopes* passing by. A total of 10 hours of footage was obtained, and cut down to 10 instances of the squid feeding or drifting. The results of the squid tracking algorithm are shown in Fig. 9 and Fig. 10 for two of the longer feeding videos.

1) Feeding Squid Footage 1 - The first feeding footage analyzed was approximately 100 frames, and features a squid moving slowly to the right before striking and capturing its prey near the end of the video. The trajectory of the squid is shown in Fig. 9a, and its velocity and acceleration are shown in Fig. 9b and Fig. 9c, respectively. A high order least squares fit was used to smooth the position, velocity and acceleration in Fig. 9 and Fig. 10.

The squid has peak velocity of 1.56 m/s and acceleration of 3.22 m/s when the squid strikes, from frames 80-90. The squid stops moving immediately after it grabs its prey, and has deceleration of -17 m/s^2 in the final frames of Fig. 9.

(c)

Fig. 9. Footage from Squid Feeding 1. Shown in (a) is the 3-D trajectory of squid with the ROV located at the origin. In (b), the smoothed velocity of squid within the x-y plane. In (c), the smoothed acceleration of squid is shown.

2) Feeding Squid Footage 2 - The second feeding footage analyzed was approximately 60 frames and featured a squid blending in with sand and accelerating toward the camera to feed, before slowly retreating back to its starting position. The brightness-based blob tracking algorithm had difficulties differentiating between the squid and sand in this video, and the particle filter lost track of the squid for several frames.

However, the resampling method of the particle filter was robust enough to recover within five frames and correctly track the squid thereafter. The 3-D trajectory of the squid is shown in Fig. 10a with the incorrectly tracked state estimates labeled. The squid's velocity and acceleration are shown in Fig. 10b and Fig. 10c, respectively. The peak velocity of 7.63 m/s and peak acceleration of 90.8 m/s^2 occur near the beginning of the video, when the squid captures its prey.

TABLE II.   SQUID MOVEMENT DURING FEEDING

|	Total Distance (m)	Mean Velocity (m/s)	Max Velocity (m/s)	Mean Pos. Accel. (m/s^2)	Max Accel. (m/s^2)
Squid footage 1	1.43	0.45	1.56	0.78	3.22
Squid footage 2	4.34	3.16	7.63	14.89	90.8

VI.   CONCLUSIONS AND FUTURE WORK

The state estimation algorithm described above is robust and easy to implement, and could be used to find the trajectory, velocity, and acceleration of squid or other small marine animals. The positions in the X and Y direction had errors less than 0.05 m, so the tracking data can be accurately used to characterize the X-Y motion of *E. scolopes* during feeding. With a more robust method of obtaining the squid's width, the method for obtaining the Z motion of the squid was shown to also work well, with errors less than 0.1 m.

The next step to improving the overall state estimate of the squid would be to incorporate a stereo-vision camera system on the ROV. The monocular vision system cannot provide accurate range information due to its dependence on and sensitivity to the measured width of the squid. The squid's width cannot be measured accurately because of the poor resolution of the underwater video footage received by the ROV, the sudden changes in the shape of the blobs in the binary image, and the varying orientation and size of the squid itself. A stereovision system would be able to provide range information without relying on blob tracking, and, together with the current state estimator in the X-Y plane, would provide a complete and accurate squid state.

A further improvement to the tracking system that has already begun involves tagging the squid with an LED, and placing LED beacons around the squid so that the ROV can localize itself and the squid relative to the stationary beacons. With this method, absolute coordinates of the squid's position could be obtained even while the ROV is in motion, allowing a researcher to more easily obtain footage of the squid.
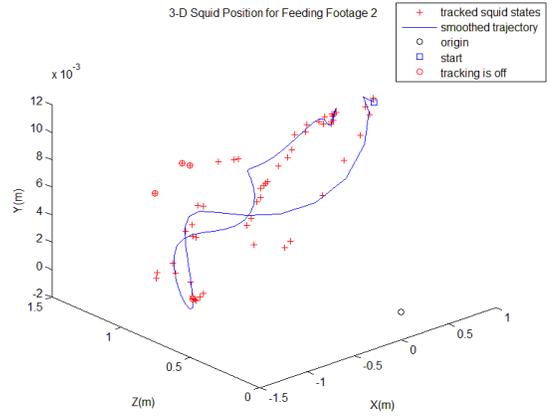
(a)
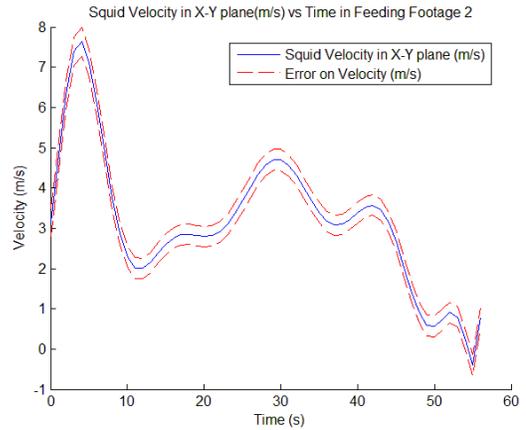
(b)
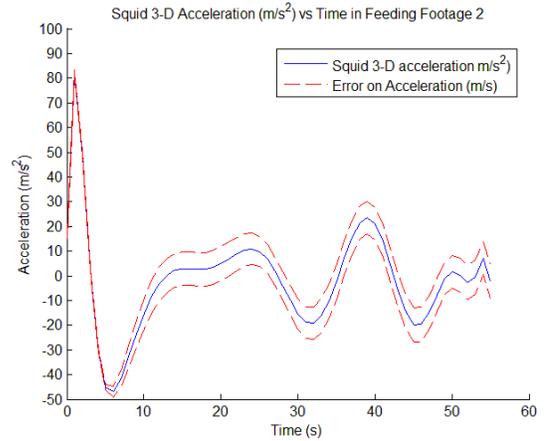
(c)

Fig. 10. Footage from Squid Feeding 2. Shown in (a) is the 3-D trajectory of squid with the ROV located at the origin. In (b), the smoothed velocity of squid within the x-y plane. In (c), the smoothed acceleration of squid is shown.

REFERENCES

[1] Hanlon, R.T., Claes, M.F., Ashcraft, S.E., and P.V. Dunlap. Laboratory culture of the sepiolid squid *Euprymna scolopes*: A model system for bacteria-animal symbiosis. Biol. Bull. 192: 364-374, 1997

[2] Nyholm, S. V., M. J. McFall-Ngai.. The Winnowing: Establishing the Squid-*Vibrio* Symbiosis. Nat. Rev. Microbiol., 2(8):632-42, 2004

[3] Fidopiastis, P.M., Boletzky, S.v., and E.G. Ruby. A new niche for *Vibrio logei*, the predominant light organ symbiont of squids in the genus *Sepiola*. J. Bacteriol. 180: 59-64,1998

[4] Laval, B., Bird, J. S., and Helland, P.D., An Autonomous Underwater Vehicle for the Study of Small Lakes, *Journal of Atmospheric and Oceanic Technology*, Vol 17, pp 69-76, January 2000.

[5] Kraeutner P. H., and Bird, J. S., Principle Components Array Processing for Swath Acoustic Mapping, Oceans '97, Halifax, Nova Scotia, October 6-9, 1997.

[6] Fleischer, S. D., Wang, H. H., Rock, S. M., and Lee, M. J., Video Mosaicking Along Arbitrary Vehicle Paths, Proc. of the Symposium on Autonomous Underwater Vehicle Technology, 293-299, Monterey, CA, June 1996.

[7] Kondo, H., Maki, T., Ura, T., Nose, Y., Sakamaki, T., and Inaishi, M., Relative Navigation of an Autonomous Underwater Vehicle Using a Light-Section Profiling System, *Proc. of the IEEE/RSJ Conference on Intelligent Robots and Systems*, 2004.

[8] Duleov, V., Scherbatyuk, A., and Jiltsova, L., Investigation of Bottom Habitant Diversity in Great Peter Bay Using Semi AUV TSL., *Proc. of IEEE Oceans Conference*, 182-187, 2003.

[9] Blackwell, S., Case, J., Glenn, S., Kohut, J., Moline, M. A., Purcell,M., Schofield, O., and VonAlt, C., A new AUV platform for studying near shore bioluminescence structure. Proc. of the 12th International Symposium on Bioluminescence and Chemiluminescence, Herring, P. J., L. J. Kricka and P. E. Stanley, editors. World Scientific, London, pp. 197-200, 2002.

[10] Rife, J., and Rock, S., Field experiments in the control of a jellyfish tracking ROV, *Proc. of the IEEE OCEANS Conference*, 2031-2038, 2002.

[11] Forney, C., Manii, E., Farris, M., Lowe, C.G, and Clark, C.M. Tracking of a Tagged Leopard Shark with an AUV: Sensor Calibration and State Estimation*, Proc. of the IEEE International Conference on Robotics and Automation (ICRA)*, 2002.

[12] Clark, C.M., Forney, C., Manii, E., Shinzaki, D., Farris, M., and Lowe, C.G., Tracking and Following of a Tagged Leopard Shark with an Autonomous Underwater Vehicle, *To appear in the Journal of Field Robotics*, 2013.

[13] Widder E., Kocak, D., and da Vitoria Lobo, N., Computer vision techniques for quantifying, tracking, and identifying bioluminescent plankton, *IEEE Journal of Oceanic Engineering*, 24, 1999.

[14] Fan, Y., and Balasuriya, A., Autonomous target tracking by auvs using dynamic vision, Proc. of the 2000 *International Symposium on Underwater Technology*, 197-192, 2000.

[15] Tang, X., and Stewart, W.K., Plankton image Classification using novel parallel-training learning vector quantization network, *Proc. of the IEEE/MTS OCEANS* '96, volume 3:1227-1236, 1996.

[16] Zhou, J., Clark, C. and J. Huissoon, SIFT Approach Used in Fish Tracking for Autonomous Underwater Vehicle, *Proc. of the 2007 International Symposium on Unmanned Untethered Submersible Technology (UUST)*, 2007.

[17] Haralick, R.M., and Shapiro, L.G., Image Segmentation Techniques, *Computer Vision, Graphics, and Image Processing,* Vol 29, Issue 1, 100-132, 1985.

[18] Pal, N.R., and Pal, S.K., A Review on Image Segmentation Techniques, *Pattern Recognition*, Vol 26, Issue 9, 1277-1294, 1993.

[19] Mihaylova, L., Brasnett, P., Canagarajah, N., & Bull, D. Object Tracking by Particle Filtering Techniques in Video Sequences. *Advances and Challenges in Multisensor Data and Information,* 260-268, 2007

[20] Thrun. S., Burgard W., and Fox, Dieter., Probabilistic Robotics. *In Probabilistic Robotics (Intelligent Robotics and Autonomous Agents),* USA, pp. 96-113, Sep 2005. The MIT Press.